

(brine, 30 mL), dried, and evaporated. The colorless powder (16, 0.75 g) was dissolved in pyridine (7 mL), cooled to 0 °C, treated with benzoyl chloride (0.92 mL, 1.11 g, 7.9 mmol), and stirred at ambient temperature for 1 h. The solution was evaporated in vacuo (<25 °C) and the residue coevaporated (EtOAc, 3 × 10 mL) and flash chromatographed (EtOAc/hexane (3:7)) to give colorless amorphous 17 (0.69 g, 60%): UV max 273, 250, 224 nm ( $\epsilon$  19 700, 24 500, 33 900);  $^1\text{H NMR}$  ( $\text{CDCl}_3$ )  $\delta$  0.15 (s, 3, SiMe), 0.17 (s, 3, SiMe), 0.90 (s, 9, SiCMe<sub>3</sub>), 2.37 (s, 3, ArMe), 4.00 (dt,  $J_{4-3} = 6.4$  Hz,  $J_{4-5'} \cong J_{4-5''} = 3.4$  Hz, 1, H4'), 4.24 (d, 2, H5',5''), 4.95 (d"q",  $J_{3-4} = 1.6$  Hz, 1, H3'), 5.33 (s, 1, CH<sub>A</sub>H<sub>B</sub>), 5.48 (s, 1, CH<sub>A</sub>H<sub>B</sub>), 6.70 ("q",  $J = 1.4$  Hz, 1, H1'), 7.20–8.10 (m, 14, ArH), 8.18 (s, 1, H2), 8.60 (s, 1, H8); MS  $m/z$  568 (2, M – OTs), 342 (15, B), 223 (100, M – TsOH – BH<sub>2</sub>). Anal. Calcd for C<sub>17</sub>H<sub>25</sub>N<sub>5</sub>O<sub>2</sub>Si: C, 61.68; H, 5.59; N, 9.47. Found: C, 61.70; H, 5.59; N, 9.47.

**6-*N,N*-Dibenzoyl-9-(3-*O*-(*tert*-butyldimethylsilyl)-2,5-dideoxy-5-iodo-2-methylene- $\beta$ -D-erythro-pentofuranosyl)-adenine (18).** A mixture of 17 (0.67 g, 0.90 mmol), dry NaI (0.50 g, 3.3 mmol), and dry Me<sub>2</sub>CO (16 mL) was refluxed for 20 h while protected from light. Solvent was evaporated and the residue partitioned (5% NaHSO<sub>3</sub>/H<sub>2</sub>O (30 mL)/CHCl<sub>3</sub> (50 mL)). The organic layer was washed (5% NaHSO<sub>3</sub>/H<sub>2</sub>O (2 × 20 mL)) and the combined aqueous phase back-extracted (CHCl<sub>3</sub> (2 × 30 mL)). The combined organic phase was dried, evaporated, and flash chromatographed (EtOAc/hexane, (7:3)) to give colorless amorphous 18 (0.34 g, 54%): UV max 274, 250 nm;  $^1\text{H NMR}$  ( $\text{CDCl}_3$ )  $\delta$  0.17 (s, 3, SiMe), 0.19 (s, 3, SiMe), 0.92 (s, 9, SiCMe<sub>3</sub>), 3.38 (dd,  $J_{5-5''} = 12.4$  Hz,  $J_{5-4} = 5.0$  Hz, 1, H5'), 3.57 (m, 2, H4',5''), 4.76 (d"q",  $J_{3-4} = 6.2$  Hz,  $J_{3-4} = 1.6$  Hz, 1, H3'), 5.38 (s, 1, CH<sub>A</sub>H<sub>B</sub>), 5.48 (dd,  $J = 2.0, 1.6$  Hz, 1, CH<sub>A</sub>H<sub>B</sub>), 6.79 ("q",  $J = 1.6$  Hz, 1, H1'), 7.30–7.90 (m, 10, ArH), 8.31 (s, 1, H2), 8.65 (s, 1, H8); MS  $m/z$  637 (1, M – 1 – CMe<sub>3</sub>), 239 (12, AdeBz).

**9-(3-*O*-(*tert*-Butyldimethylsilyl)-2,5-dideoxy-2-methylene- $\beta$ -D-glycero-pent-4-enofuranosyl)adenine (21).** DBN (70  $\mu\text{L}$ , 70 mg, 0.56 mmol) in DMF (0.25 mL) was added to a solution of 18 (0.20 g, 0.28 mmol) in DMF (4 mL) at 0 °C. The mixture was stirred at ambient temperature for 2 h, and additional DBN (70  $\mu\text{L}$ , 70 mg, 0.56 mmol) in DMF (0.25 mL) added. After 1.5 h, NH<sub>3</sub>/MeOH (17 mL) was added, stirring continued at ambient temperature for 18 h, and the mixture evaporated in vacuo. The residue was flash chromatographed (EtOAc/hexane, (4:1)) to give a light yellow powder (34 mg) whose  $^1\text{H NMR}$  spectrum indicated a mixture (~4:1, respectively) of 21 [ $^1\text{H NMR}$  ( $\text{CDCl}_3$ )  $\delta$  0.18, 0.19 (2s, 6, SiMe<sub>2</sub>), 0.97 (s, 9, SiCMe<sub>3</sub>), 4.28 (dd,  $J_{5-5''} = 2.2$  Hz,  $J_{5-3'} = 1.6$  Hz, 1, H5'), 4.53 (t,  $J_{5'-3'} = 2.2$  Hz, 1, H5''), 5.40 (s, 1, CH<sub>A</sub>H<sub>B</sub>), 5.53 (m, 1, H3'), 5.56 (s, 1,

CH<sub>A</sub>H<sub>B</sub>), 5.73 (br s, 2, NH<sub>2</sub>), 6.78 ("q",  $J = 1.6$  Hz, 1, H1'), 7.80 (s, 1, H2), 8.33 (s, 1, H8)] and the debenzoylated 5'-iodo starting material [ $^1\text{H NMR}$  ( $\text{CDCl}_3$ )  $\delta$  0.15, 0.17 (2s, 6, SiMe<sub>2</sub>), 0.95 (s, 9, SiMe<sub>3</sub>), 3.40–3.60 (m, 3, H4',5',5''), 4.78 (d"q",  $J_{3-4} = 6.0$  Hz,  $J_{3-4} = 2.0$  Hz, 1, H3'), 5.30 (t,  $J = 1.7$  Hz, 1, CH<sub>A</sub>H<sub>B</sub>), 5.45 (t,  $J = 2.0$  Hz, 1, CH<sub>A</sub>H<sub>B</sub>), 5.73 (br s, 2, NH<sub>2</sub>), 6.74 ("q",  $J = 1.7$  Hz, 1, H1'), 7.83 (s, 1, H2), 8.40 (s, 1, H8)]. Lower yields of 21 resulted from extended treatment with DBN.

**9-(2,5-Dideoxy-2-methylene- $\beta$ -D-glycero-pent-4-enofuranosyl)adenine (4',5'-Didehydro-2',5'-dideoxy-2'-methyleneadenosine) (22).** TBAF/THF (1 M; 0.1 mL, 0.1 mmol) was added to the above mixture (21 and the 5'-iodo compound; 34 mg, ~0.09 mmol) in THF (1.5 mL) at 0 °C, and stirring was continued at 0 °C for 30 min. Solvent was evaporated (<20 °C) and the residue flash chromatographed (MeOH/CH<sub>2</sub>Cl<sub>2</sub> (7:93)) to give a light yellow viscous oil (12 mg) that contained 22 and the deprotected 5'-iodo compound (~4:1). Preparative HPLC (C<sub>18</sub>; CH<sub>3</sub>CN/H<sub>2</sub>O (1:4)) and crystallization (MeOH/Et<sub>2</sub>O) gave pale yellow solid 22 (6 mg): mp 137–138 °C; UV (H<sub>2</sub>O, pH 7) max 260 nm ( $\epsilon$  14 600);  $^1\text{H NMR}$  (Me<sub>2</sub>SO-*d*<sub>6</sub>)  $\delta$  4.20 (s, 1, H5'), 4.33 (s, 1, H5''), 5.43 (s, 1, CH<sub>A</sub>H<sub>B</sub>), 5.51 (s, 1, CH<sub>A</sub>H<sub>B</sub>), 5.61 (s, 1, H3'), 6.10 (br s, 1, OH3'), 6.89 (s, 1, H1'), 7.31 (br s, 2, NH<sub>2</sub>), 8.13 (s, 1, H2), 8.25 (s, 1, H8); MS  $m/z$  245 (30, M<sup>+</sup>), 203 (10, M – C<sub>2</sub>H<sub>5</sub>O), 134 (90, B), 110 (30, M – BH), 84 (100, M – B – C<sub>2</sub>H<sub>5</sub>). Anal. Calcd for C<sub>11</sub>H<sub>11</sub>N<sub>5</sub>O<sub>2</sub>: C, 53.87; H, 4.52; N, 28.56. Found: C, 53.47; H, 4.80; N, 28.22.

The 2',5'-dideoxy-5'-iodo-2'-methyleneadenosine (2 mg) had  $^1\text{H NMR}$  (Me<sub>2</sub>SO-*d*<sub>6</sub>)  $\delta$  3.43 (dd,  $J_{5-5''} = 10.0$  Hz,  $J_{5-4} = 6.2$  Hz, 1, H5'), 3.60–3.70 (m, 2, H4',5''), 4.78 (br m, 1, H3'), 5.23 (dd,  $J = 2.0, 1.7$  Hz, 1, CH<sub>A</sub>H<sub>B</sub>), 5.42 (t,  $J = 2.0$  Hz, 1, CH<sub>A</sub>H<sub>B</sub>), 5.95 (br d,  $J = 5.0$  Hz, 1, OH3'), 6.66 (m,  $J = 1.7$  Hz, 1, H1'), 7.32 (br s, 2, NH<sub>2</sub>), 8.15 (s, 1, H2), 8.23 (s, 1, H8).

**Acknowledgment.** We thank the American Cancer Society (Grant No. CH-405) for generous support and Mrs. Kathryn M. Rollins for assistance with the manuscript.

**Registry No.** 2a, 65109-11-7; 2b, 69504-03-6; 2c, 64911-28-0; 2d, 69304-45-6; 3, 86734-95-4; 4, 90813-59-5; 5, 90318-44-8; 6, 137058-76-5; 7, 78151-96-9; 8, 137058-77-6; 9, 137058-78-7; 10, 104409-40-7; 11, 104409-41-8; 12, 137058-79-8; 13, 137058-80-1; 14, 137058-81-2; 15, 137058-82-3; 15 3'-tosyl derivative, 137058-89-0; 16, 137058-83-4; 17, 137091-53-3; 18, 137058-84-5; 18 debenzoylated derivative, 137058-90-3; 18 debenzoylated desilylated derivative, 137058-91-4; 19, 137058-85-6; 20, 137058-86-7; 21, 137058-87-8; 22, 137058-88-9; SAHase, 9025-54-1; RDPR, 9047-64-7.

## Electrochemical and Enzyme-Mediated Oxidations of Tetrahydropapaveroline

Fa Zhang and Glenn Dryhurst\*

Department of Chemistry and Biochemistry, University of Oklahoma, Norman, Oklahoma 73019-0370

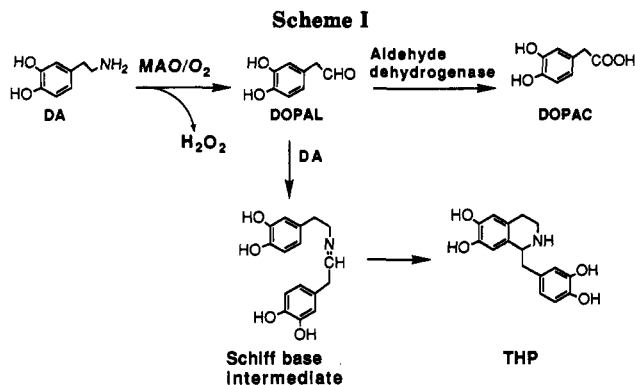
Received April 5, 1991 (Revised Manuscript Received August 9, 1991)

The electrochemically driven and enzyme-mediated oxidations of the alkaloid tetrahydropapaveroline (THP) have been studied in aqueous solution. The electrochemical oxidation of THP is a 4e/4H<sup>+</sup> reaction giving diquinone 6 as the intermediate. In the absence of strong nucleophiles 6 undergoes an internal Michael reaction to give 5,6-dihydrodibenz[b,g]indolizine-2,3,9,10-tetrol (2) as the initial isolated product. Ceruloplasmin/O<sub>2</sub>, peroxidase/H<sub>2</sub>O<sub>2</sub>, and tyrosinase/O<sub>2</sub> all cause a very rapid oxidation of THP to give 2. In the presence of the intraneuronal nucleophile glutathione putative diquinone intermediate 6 reacts to give 1,2,3,4-tetrahydro-1-[(6-*S*-glutathionyl-3,4-dihydroxyphenyl)methyl]-6,7-isoquinolinediol (5). The latter conjugate can be further oxidized and attacked by a second molecule of glutathione to give 1,2,3,4-tetrahydro-[6-*S*-glutathionyl-3,4-dihydroxyphenyl)methyl]-8-*S*-glutathionyl-6,7-isoquinolinediol (4) and 1,2,3,4-tetrahydro-1-[(6-*S*-glutathionyl-3,4-dihydroxyphenyl)methyl]-5-*S*-glutathionyl-6,7-isoquinolinediol (3). The possible role of the oxidation of THP in the neurodegenerative aspects of chronic alcoholism are discussed.

The normal metabolism of the catecholaminergic neurotransmitter dopamine (DA) in the central nervous sys-

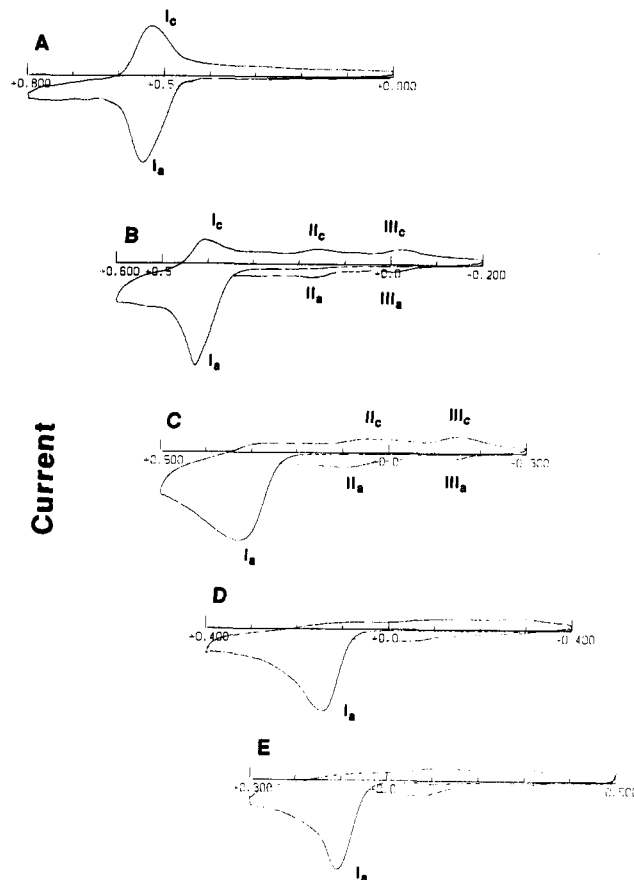
tem is initiated by monoamine oxidase (MAO) which catalyzes oxidative deamination of the transmitter to 3,4-dihydroxyphenylacetaldehyde (DOPAL). Subsequently, DOPAL is rapidly oxidized in the presence of

\* Author to whom correspondence should be addressed.



aldehyde dehydrogenase to 3,4-dihydroxyphenylacetic acid (DOPAC) (Scheme I). More than two decades ago Davis and Walsh<sup>1</sup> proposed that heavy consumption of ethanol might cause a diversion of this metabolism because of the competitive inhibition of aldehyde dehydrogenase by the proximate metabolite of ethanol, acetaldehyde. As a result, a nonenzymatic condensation was speculated to occur between DOPAL and DA to produce the alkaloid tetrahydropapaveroline (THP) (Scheme I). It was further suggested that THP might have addictive liability or be further metabolized to morphine-like compounds which are responsible for the syndrome of alcohol addiction. While this hypothesis initially generated considerable controversy<sup>2,3</sup> it was subsequently found that chronic intracerebroventricular (i.c.v.) infusions of THP to the rat evoked a dramatic increase in the preference of the animal for ethanol consumption.<sup>4</sup> Furthermore, this effect persisted long after drug administration had been terminated. These observations appear to provide significant support for the Davis and Walsh hypothesis.<sup>1</sup> However, the evidence for the presence of THP in brain tissue or of urine of humans after ethanol consumption is scientifically weak.<sup>5</sup> This might be a consequence of the short half-life of the alkaloid in the brain (17.3 min in rat brain).<sup>6</sup> Furthermore, THP is rapidly converted in vivo by the rat and in vitro by rat brain preparations into tetrahydroprotoberbine alkaloids.<sup>7</sup> The trace levels of the latter alkaloids detected, however, suggest that other metabolic transformations must occur although the resulting products have not been identified.<sup>7</sup>

Long-term heavy consumption of ethanol not only has addictive and behavioral consequences but also results in impaired learning ability and memory and a general decline of intellectual abilities, all of which have been attributed to organic brain damage.<sup>8</sup> Loss of neurons, particularly in hippocampal regions of the brain, has been observed.<sup>9</sup> Indeed, the effects of chronic alcoholism have been likened to a premature aging of the brain.<sup>10</sup> Recently, a hypothesis was advanced which proposes that oxidation reactions of various tetrahydroisoquinoline (TIQ) alkaloids elevated in the brain following heavy ethanol



### Potential/Volt vs.SCE

**Figure 1.** Cyclic voltammograms at the PGE of 0.295 mM tetrahydropapaveroline (THP) in phosphate buffers ( $\mu = 0.5$ ) at (A) pH 1.5, (B) pH 3.0, (C) pH 5.0, (D) pH 7.0, and (E) pH 9.2. Sweep rate: 100 mV s<sup>-1</sup>.

consumption might lead to toxins which are responsible for neuronal damage.<sup>11</sup> However, little is currently known about the oxidative chemistry and biochemistry of THP or other endogenous TIQ alkaloids.

It is also of interest to note that L-DOPA treated Parkinson's disease patients excrete THP and, following ethanol consumption, there might be a further increase in the output of the alkaloid.<sup>12</sup> THP has also been detected in brain following the administration of large doses of L-DOPA.<sup>13</sup> There have been suggestions that the marked elevations of THP (and perhaps other TIQ alkaloids) during L-DOPA therapy for Parkinson's disease might be associated with various unusual discrepancies associated with this treatment.<sup>14</sup> For example, i.c.v. administration of THP to rat causes behavioral effects<sup>15</sup> which are also evoked by L-DOPA.<sup>16</sup> It has also been speculated that the "on-off" effects of L-DOPA therapy are related to the TIQ alkaloids which are formed.<sup>17</sup> Thus, an argument can be advanced that THP, elevated as a result of L-DOPA therapy, might play a neuropathological role in the etiology of Parkinson's disease under this drug regimen. It is

(1) Davis, V. E.; Walsh, M. J. *Science* 1970, 167, 1005-1007.  
 (2) Seevers, M. H. *Science* 1970, 170, 1113-1114.  
 (3) Halushka, P. V.; Hoffmann, P. C. *Science* 1970, 169, 1104-1105.  
 (4) Myers, R. D.; Melchior, C. L. *Science* 1977, 196, 554-556.  
 (5) Collins, M. A. In *Biological Effects of Alcohol*; Bergleiter, H., Ed.; Plenum Press: New York, 1980; pp 87-102.  
 (6) Melchior, C. L.; Deitrich, R. A. In *Biological Effects of Alcohol*; Bergleiter, H., Ed.; Plenum Press: New York, 1980; pp 121-129.  
 (7) Davis, V. E.; Cashaw, H. L.; McMurtrey, K. D. In *Alcohol Intoxication and Withdrawal*; Gross, M. M., Ed.; Plenum Press: New York, 1975; pp 65-78.  
 (8) Freund, G. *Ann. Rev. Pharmacol.* 1973, 13, 217-227.  
 (9) Walker, D. W.; Barnes, D. E.; Zornetzer, S. F.; Hunter, B. E.; Kubanis, P. *Science* 1980, 209, 711-712.  
 (10) Ryan, C.; Butters, N. *Alc. Clin. Exp. Res.* 1980, 4, 288-293.

(11) Collins, M. A. *Trends Pharm. Sci.* 1982, 3, 373-375.  
 (12) Sandler, M.; Bonham-Carter, S.; Hunter, K. R.; Stern, G. *Nature* 1973, 241, 439-443.  
 (13) Turner, A. J.; Baker, K. M.; Algeri, S.; Frigorio, A.; Garattini, S. *Life Sci.* 1974, 14, 2247-2257.  
 (14) Sourkes, T. L. *Nature* 1971, 229, 413-414.  
 (15) Awazi, N.; Goldberg, H. C. *Naunyn-Schmiedeberg's Arch. Pharmacol.* 1979, 306, 135-146.  
 (16) Butcher, L. L.; Engel, J. *Brain Res.* 1969, 15, 233-242.  
 (17) Hornykiewicz, O. *Fed. Proc.* 1971, 32, 183-190.

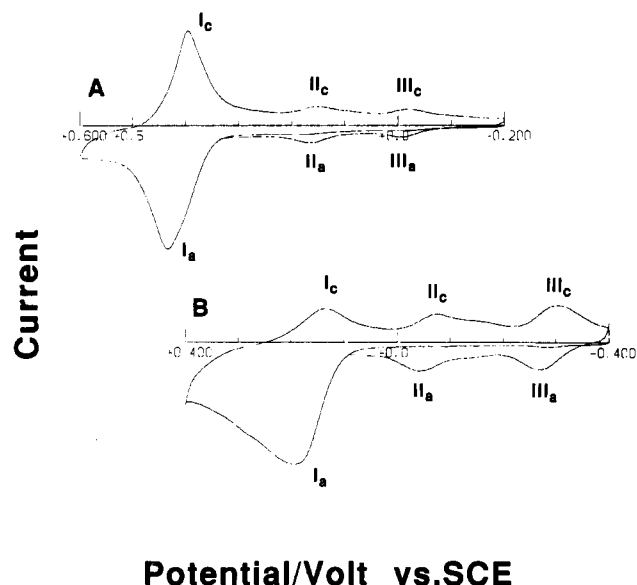


**Figure 2.** Cyclic voltammograms at the PGE of 0.295 mM tetrahydropapaveroline (THP) in phosphate buffers at (A) pH 3.0 and (B) pH 7.0. Sweep rate: (A) 500  $\text{mV s}^{-1}$ , (B) 5000  $\text{mV s}^{-1}$ .

known, for example, that large, acute i.c.v. injections of THP to rats cause death<sup>15</sup> although the mechanisms involved are unknown.

The objectives of the work described in this paper were to investigate the basic oxidation chemistry and biochemistry of THP, to characterize key intermediates, and to isolate the major oxidation products. Electrochemical approaches were initially employed to study the oxidation reactions of THP because such techniques can be used to study oxidation reactions over a very wide range of experimental conditions. Various enzyme-mediated oxidations of THP have also been studied. The potential roles of oxidations of THP in neurodegenerative processes are discussed.

## Results

**Voltammetric Studies.** Representative cyclic voltammograms of THP obtained between pH 1.5 and 9.2 are shown in Figure 1. On the initial anodic sweep a single oxidation peak  $I_a$  appears. After scan reversal, at pH 1.5, reversible reduction peak  $I_c$  appears, the peak current ( $i_p$ ) for which is approximately equal to that of oxidation peak  $I_a$  at a sweep rate ( $\nu$ ) of 100  $\text{mV s}^{-1}$  (Figure 1A). However, with increasing pH, reduction peak  $I_c$  systematically decreases and at pH  $\geq 5$  disappears (Figure 1B–E). Correspondingly, two broad, apparently reversible couples characterized by peaks  $II_c/II_a$  and  $III_c/III_a$  appear. At slow sweep rates and pH  $\geq 7$  the latter couples are poorly defined. However, cyclic voltammograms at pH 3 and 7, for example, at larger values of  $\nu$  reveal that reduction peak  $I_c$  can be observed and that the peaks  $II_c/II_a$  and  $III_c/III_a$  couples are better defined (Figure 2). At sufficiently large values of  $\nu$  (e.g., 50  $\text{V s}^{-1}$ ) at pH 3.0 the  $i_p$  values for peaks  $I_c$  and  $I_a$  become the same and the peaks  $II_c/II_a$  and  $III_c/III_a$  couples disappear. However, at pH 7, even at  $\nu = 100 \text{ V s}^{-1}$ , the latter couples can still be observed but  $i_p$  for peak  $I_c$  is smaller than that for peak  $I_a$ . Over the pH range studied (1.5–9.2) the pattern of cyclic voltammetric behaviors is independent of the concentration of THP (59  $\mu\text{M}$  to 0.6 mM).

The peak potential ( $E_p$ ) for peak  $I_a$  shifts linearly to more negative potentials according to the expression:

$$E_{p(\text{pH}1.5-9.2)} = [0.62 - 0.06 \text{ pH}] \text{ V}$$

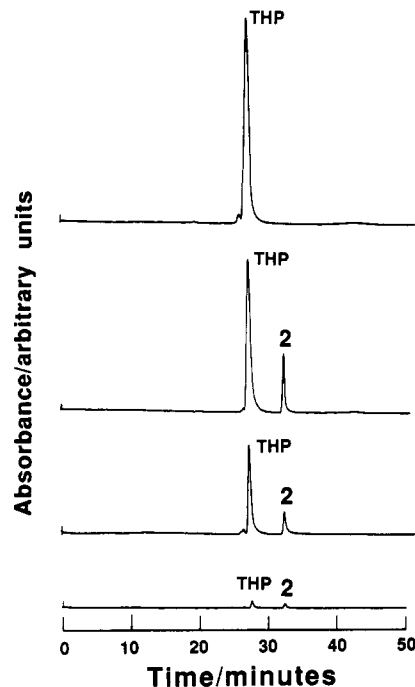


**Figure 3.** HPLC chromatograms of the solution obtained when 0.64 mM tetrahydropapaveroline (THP) was electrolyzed at 0.46 V in pH 3.0 phosphate buffer ( $\mu = 0.15$ ) for (A) 0, (B) 20, (C) 75, and (D) 270 min. Injection volume: 2 mL. Chromatography employed HPLC method I.

Thus, at pH 7.0  $E_p$  is +0.20 V indicating that THP is a relatively easily oxidized compound.

The peak current function ( $i_p/AC\nu^{1/2}$ , where all terms have their usual electrochemical significance) increased significantly with increasing  $\nu$  (measured at pH 3.0 and 7.0). The values of  $i_p/C\nu^{1/2}$  decreased systematically with increasing concentrations ( $C$ ) of THP. Such behaviors are indicative of strong adsorption of THP at the surface of the PGE.<sup>18</sup>

**Controlled Potential Electrooxidation and Product Characterization.** Controlled-potential electrooxidations of THP at pH 1.5, 3.0, and 7.0 at potentials close to  $E_p$  for oxidation peak  $I_a$  caused the initially colorless solution to become pale pink. Representative chromatograms obtained on the product solution following electrooxidation of THP (0.64 mM) in pH 3.0 phosphate buffer are shown in Figure 3; electrolyses at pH 1.5, 5.0, and 7.0 gave identical chromatographic behaviors. During the first few minutes of the electrolysis THP was converted into a single major product, 2. However, following the initial growth of the HPLC peak of 2, both THP and 2 decreased simultaneously and ultimately disappeared; no new chromatographic peaks appeared. During the latter stages of such an electrochemical oxidation a black precipitate appeared which was not soluble in any common organic solvent. Compound 2 was, for the first time, isolated and spectroscopically characterized (high-resolution FAB-MS and  $^1\text{H}$  NMR) as 5,6-dihydrodibenz[*b,g*]indolizine-2,3,9,10-tetrol. The structure of 2 was confirmed by converting it to a tetraacetyl derivative.<sup>19,20</sup> Cyclic voltammograms of 2 at pH 3.0 and 7.0 are shown in Figure 4. At pH 3.0, 2 exhibits at initial oxidation peak at  $E_p = +0.38$  V. After sweep reversal, two reversible couples appear at  $E^\circ +0.15$  and  $-0.02$  V. At pH 7.0  $E_p$  for the primary oxidation peak of 2 is +0.13 V and, after scan reversal, the

(18) Wopscall, R. H.; Shain, I. *Anal. Chem.* 1967, 39, 1514–1527.

(19) Harley-Mason, J. *J. Chem. Soc.* 1953, 1465–1466.

(20) Mak, C.-P.; Brossi, A. *Heterocycles* 1979, 12, 1413–1415.

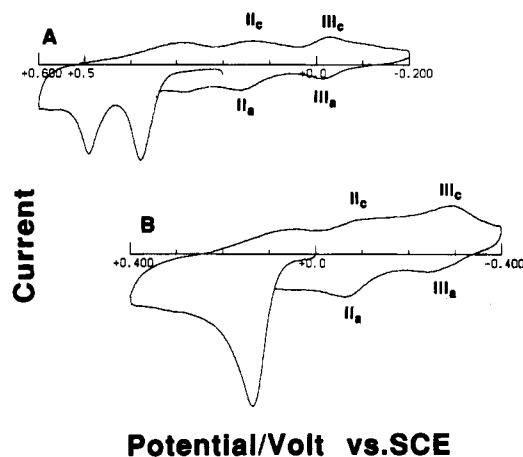


**Figure 4.** Cyclic voltammograms at the PGE of 5,6-dihydrobenz[*b,g*]indolizene-2,3,9,10-tetrol in phosphate buffers at (A) pH 3.0 and (B) pH 7.0. Sweep rate: 100 mV s<sup>-1</sup>.

**Table I.** Coulometric *n* Values for the Electrochemical Oxidation of Tetrahydropapaveroline in pH 3.0 Phosphate Buffer

THP concn (mM)	applied potential <sup>a</sup> (V)	experimental <sup>b</sup> <i>n</i> value
0.18	0.40	4.58
	0.46	4.77
	0.50	4.95
0.36	0.40	4.59
	0.46	4.79
	0.50	5.80
0.72	0.40	5.76
	0.46	6.41
	0.50	6.49

<sup>a</sup>  $E_p$  for peak I<sub>a</sub> at pH 3.0 is 0.44 V. <sup>b</sup> *n* values were measured when ca. 40% of the initial THP was consumed.

two reversible couples appear at -0.07 and -0.28 V. Thus, at pH 3.0 and 7.0 the primary oxidation peak of 2 occurs at slightly more negative potentials than  $E_p$  for peak I<sub>a</sub> of THP (+0.44 and +0.20 V, respectively). The similarities between these potentials are in accord with the observation that 2 is initially formed as a product but is subsequently oxidized in parallel with THP. Furthermore, the reversible couples responsible for peaks II<sub>c</sub>/II<sub>a</sub> and III<sub>c</sub>/III<sub>a</sub> observed in cyclic voltammograms of THP (Figure 2) are observed in cyclic voltammograms of 2 (Figure 4), indicating that 2 is indeed formed and oxidized to the species responsible for the latter couples in the peak I<sub>a</sub> process. However, the peaks II<sub>c</sub>/II<sub>a</sub> and III<sub>c</sub>/III<sub>a</sub> couples are relatively small compared to peak I<sub>a</sub> at all the pH values studied (Figure 1), indicating that the peak I<sub>a</sub> oxidation of THP, at least initially, results in only a small amount of secondary oxidation of 2. No attempts were made to investigate the oxidation chemistry of 2 or to isolate the resulting oxidation products. However, it has been previously noted that 2 is easily oxidized in basic aqueous solution to a deep violet product which has been proposed to be either a dibenz[*b,g*]indolizine<sup>19</sup> or a dimer of 2.<sup>20</sup> The red color imparted to samples of 2 isolated in this study no doubt derives from its partial secondary oxidation to such products.

Strong adsorption of THP at the PGE precluded the measurement of voltammetric *n* values. However, representative coulometric *n* values, measured at pH 3.0, are given in Table I. Electrolyses of low concentrations (ca. 0.2 mM) of THP at potentials less positive than  $E_p$  for peak I<sub>a</sub> gave *n* values slightly larger than 4. Increasingly positive applied potentials resulted in a systematic increase in experimental *n* values. Increasing concentrations of

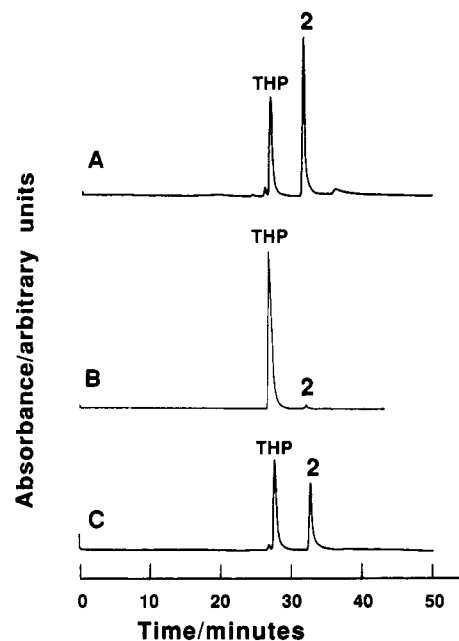


**Figure 5.** HPLC chromatograms of the product solution formed by oxidation of 0.64 mM tetrahydropapaveroline (THP) in pH 7.0 phosphate buffer ( $\mu = 0.15$ ) at  $23 \pm 2$  °C in the presence of (A) 30 units mL<sup>-1</sup> tyrosinase for 4 min, (B) 44.7 units mL<sup>-1</sup> ceruloplasmin for 50 min, and (C) type VI peroxidase (4 units mL<sup>-1</sup>) and H<sub>2</sub>O<sub>2</sub> (0.5 mM) for 1 min. Injection volume: 2 mL. Chromatography employed HPLC method I.

THP also resulted in an increase in the measured *n* value. The data presented in Table I suggest that under coulometric conditions the initial *n* value is 4, but increasingly positive applied potentials cause this value to increase as a result of secondary oxidation of 2. Electrolyses of higher THP concentrations required longer times than electrolyses of low concentrations; hence, presumably, permitting more extensive secondary oxidation reactions. Coulometric data obtained at pH 1.5 and 7.0 were very similar to those obtained at pH 3.0.

**Enzyme-Mediated Oxidations of THP.** In the absence of an enzyme catalyst THP is autoxidized very slowly in pH 7.0 phosphate buffer ( $\mu = 0.15$ ). However, after 10 h in a stirred solution (pH 7.0;  $23 \pm 2$  °C) approximately 5% of THP (0.64 mM) was converted to 2. Tyrosinase/O<sub>2</sub>, ceruloplasmin/O<sub>2</sub>, and peroxidase/H<sub>2</sub>O<sub>2</sub> all caused a very rapid oxidation of THP to 2 (Figure 5). In the absence of H<sub>2</sub>O<sub>2</sub>, peroxidase had no catalytic effect on the oxidation of THP. The chromatograms shown in Figure 5 were recorded after only very short periods of oxidation of THP. When the reactions were permitted to proceed for a longer period of time, the chromatographic peaks of THP and 2 decreased and disappeared and a black precipitate was formed in the solution.

**Effects of Glutathione on the Oxidation of THP.** Cyclic voltammograms of THP indicated that the peak I<sub>a</sub> oxidation results in the formation of a reversibly reduced proximate oxidation product characterized by reduction peak I<sub>c</sub> (Figure 2). The lifetime of this proximate product is appreciably longer at pH ≤ 3 than at pH ≥ 7 (compare Figures 1 and 2). Coulometric measurements suggested that the initial electrode reaction is a 4e process and, therefore, that the compound reduced in the peak I<sub>c</sub> electrode reaction is diquinone 6 (see later discussion). The fact that several enzyme-mediated oxidations and the electrochemically driven reaction all give 2 as the major initial isolatable product suggests that 6 is formed as an intermediate in all of these processes. Putative quinone 6 is a highly electron-deficient compound and, hence,

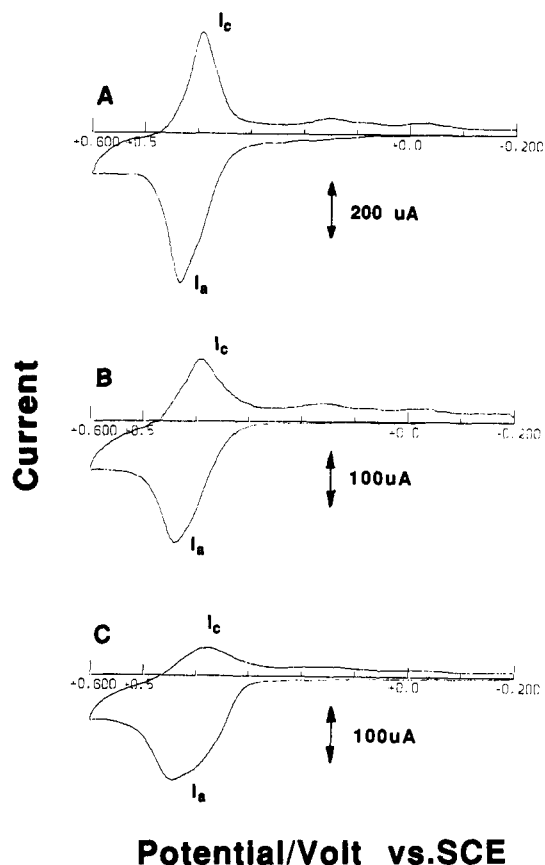


**Figure 6.** Cyclic voltammograms at the PGE of 0.285 mM tetrahydropapaveroline (THP) in pH 3.0 phosphate buffer ( $\mu = 1.0$ ) in the presence of (A) 0, (B) 1.63, and (C) 6.51 mM glutathione. Sweep rate:  $500 \text{ mV s}^{-1}$ .

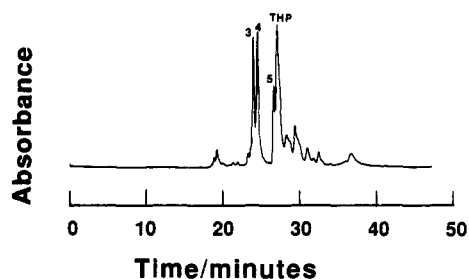


**Figure 7.** HPLC chromatograms (method I) of the product mixture formed following controlled potential electrooxidation of 0.72 mM tetrahydropapaveroline (THP) at 0.19 V in pH 7.0 phosphate buffer in the presence of 3.47 mM glutathione.

would be expected to be susceptible to attack by nucleophiles. Figure 6 shows a series of cyclic voltammograms of THP recorded in the presence of glutathione (GSH). These reveal that with increasing concentrations of GSH reduction peak  $I_c$  systematically decreases relative to oxidation peak  $I_a$ . Such results indicate that the proximate oxidation product of THP, responsible for reduction peak  $I_c$ , is attacked by GSH. Controlled potential electrooxidation of THP at peak  $I_a$  potentials in the presence of GSH at pH 7.0 resulted in the formation of 3–5 as major new products (Figure 7). Chromatograms of the product solutions obtained following the tyrosinase-mediated oxidation of THP in the presence of GSH are shown in Figure 8. Under the experimental conditions described in Figure 8 compound 2 did not appear as a product. The first product formed was the monogluthionyl adduct 5 which grew during the initial stages of the reaction and then decreased and was replaced by the two digluthionyl adducts 3 and 4. Experiments revealed that conjugate 5

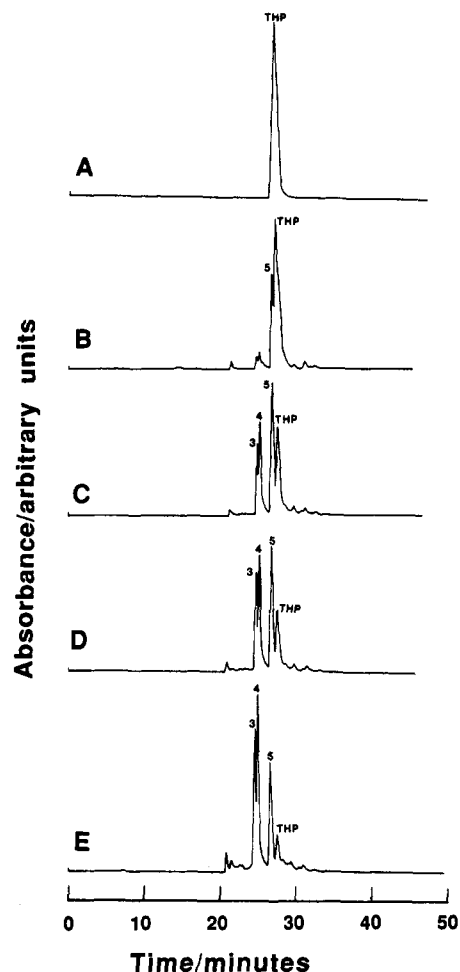


**Figure 8.** HPLC chromatograms of the product mixture formed upon oxidation of 0.64 mM tetrahydropapaveroline (THP) in pH 7.0 phosphate buffer in the presence of tyrosinase ( $30 \text{ units mL}^{-1}$ ) and glutathione ( $3.47 \text{ mM}$ ) at  $23 \pm 2 \text{ }^\circ\text{C}$  after (A) 0, (B) 5, (C) 58, (D) 115, (E) 280, and (F) 342 min. Injection volume: 2 mL. Chromatography employed HPLC method I.

is oxidized by tyrosinase/ $\text{O}_2$  in the presence of excess GSH to yield 3 and 4 in approximately equal yield. Cyclic voltammograms of glutathionyl adducts 3–5 show that all compounds are quite easily oxidized at pH 7 (Figure 9) but exhibit very complex electrochemical behaviors. In agreement with the ease of electrochemical oxidation of 3–5 it was also noted that when enzyme-mediated oxidations of THP in the presence of GSH were permitted to proceed for several hours many secondary products were formed (HPLC analysis) and the heights of the chromatographic peaks of 3–5 decreased.

**Reaction Pathways.** Cyclic voltammetry indicates that the peak  $I_a$  electrooxidation of THP generates a reversibly reducible proximate oxidation product characterized by reduction peak  $I_c$ . The lifetime of this proximate product is significantly less in the physiological pH domain than at low pH. Coulometric and voltammetric results ( $\partial E_p/\partial \text{pH} = -60 \text{ mV}$ ) support the conclusion that the initial electrode reaction is a  $4e-4H^+$  reversible oxidation of THP. The major product derived directly from the proximate oxidation product is the tetracyclic alkaloid 5,6-dihydrodibenz[*b,g*]indolizine-2,3,9,10-tetrol (2). Accordingly, it is proposed that THP is initially electrooxidized in a  $4e-4H^+$  reaction to the diquinone 6 (Scheme II) and that it is this species which is responsible for reduction peak  $I_c$  observed in cyclic voltammograms of THP. In order for 6 to ultimately form the tetracyclic alkaloid 2 a ring closure must clearly occur. However, based upon the information

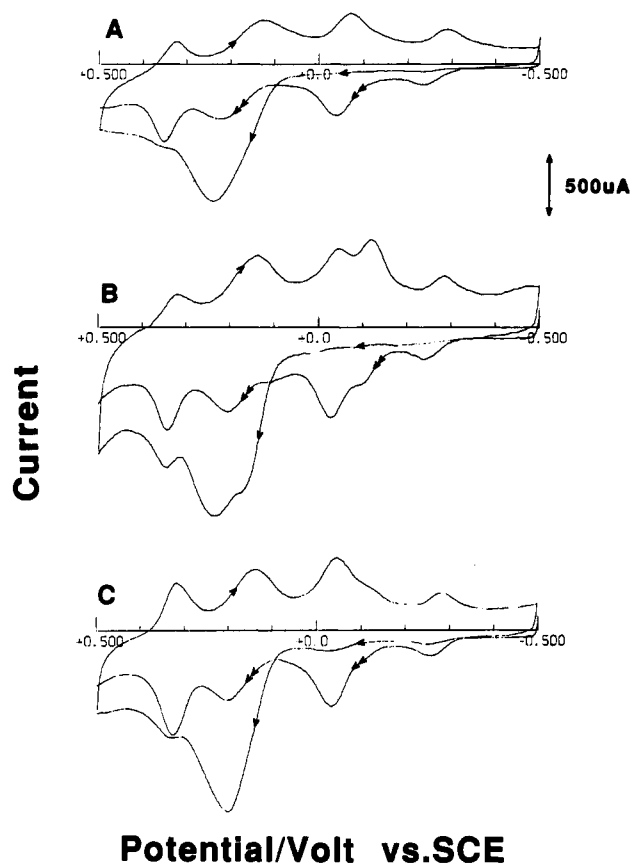
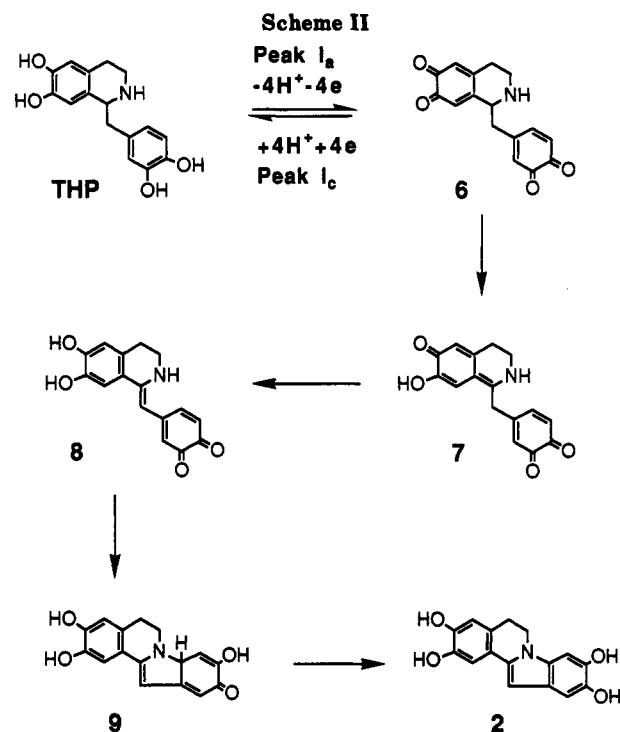


**Figure 9.** Cyclic voltammograms at the PGE of (A) 0.25 mM 5, (B) 0.23 mM 4, and (C) 0.24 mM 3 in pH 7.0 phosphate buffer ( $\mu = 1.0$ ). Sweep rate:  $5 \text{ V s}^{-1}$ .

available the exact sequence of events leading to 2 cannot presently be specified. Nevertheless, it is known that a related alkaloid, 1,2,3,4-tetrahydro-1-methyl-6,7-isouquinolinediol (salsolinol), is oxidized to a 6,7-*o*-quinone that rapidly and essentially irreversibly tautomerizes to quinone methide tautomers,<sup>21</sup> one of which has been isolated and structurally characterized. By analogy, it is proposed that 6 rapidly tautomerizes to quinone methide 7 (Scheme II). An internal Michael reaction then yields 9 and, following appropriate rearrangement, 2. Tyrosinase/ $\text{O}_2$ , ceruloplasmin/ $\text{O}_2$ , and peroxidase/ $\text{H}_2\text{O}_2$  also result in the oxidation of THP to 2. While the goal of this research was not aimed at elucidating the precise mechanistic aspects of the enzymatic oxidation of THP, it is known that tyrosinase and ceruloplasmin catalyze the oxidation of *o*-diphenols to the corresponding *o*-quinones.<sup>22,23</sup> Peroxidase/ $\text{H}_2\text{O}_2$  generally catalyzes one-electron oxidations of organic substrates to yield radical intermediates.<sup>24</sup> Nevertheless, it appears that all of the oxidative enzyme systems studied convert THP to diquinone 6, although it is very probable that somewhat different mechanistic pathways lead to this intermediate. That 6 is in fact formed in the electrochemically driven and enzyme-mediated oxidations of THP is supported by formation of glutathionyl conjugates 3–5 when these reactions are



carried out in the presence of GSH. We propose that diquinone 6 is initially attacked by GSH to give the intermediate glutathionyl conjugate 10 (Scheme III). Reduction of 10 by GSH then yields 5. Alternatively, nucleophilic attack by GSH yields the diglutathionyl conjugate 3 (Scheme III). HPLC analyses throughout the oxidation of THP in the presence of GSH (Figure 8) indicate that the monogluthionyl conjugate 5 is initially formed in high yield and then is further consumed to yield 3 and 4. Furthermore, independent studies reveal that 5 is oxidized (electrochemically and enzymatically) in the presence of GSH to give 3 and 4. Accordingly, it is apparent that 5 can be oxidized to diquinone 11 which is attacked by GSH to give 12 and 13. Reduction of these compounds by GSH yields 3 and 4, respectively (Scheme III). Evidence in support of a role for GSH as a reductant as proposed in Scheme III is provided by the fact that significant concentrations of GSSG are formed when THP is oxidized (electrochemically or enzymatically) in the presence of the tripeptide. In the absence of THP, GSH is not significantly oxidized to GSSG either electrochemically or enzymatically under the conditions employed in these experiments. It might be expected that putative quinone intermediates 12 and 13 should also be attacked by GSH to yield trisubstituted glutathionyl conjugates of THP. An inspection of the chromatograms shown in Figure 8 indicates that additional minor products are formed particularly in the latter stages of the oxidation reactions of THP in the presence of GSH. While the compounds responsible for these peaks have not been isolated and characterized they might well be due to more highly substituted glutathionyl conjugates of THP.

### Discussion

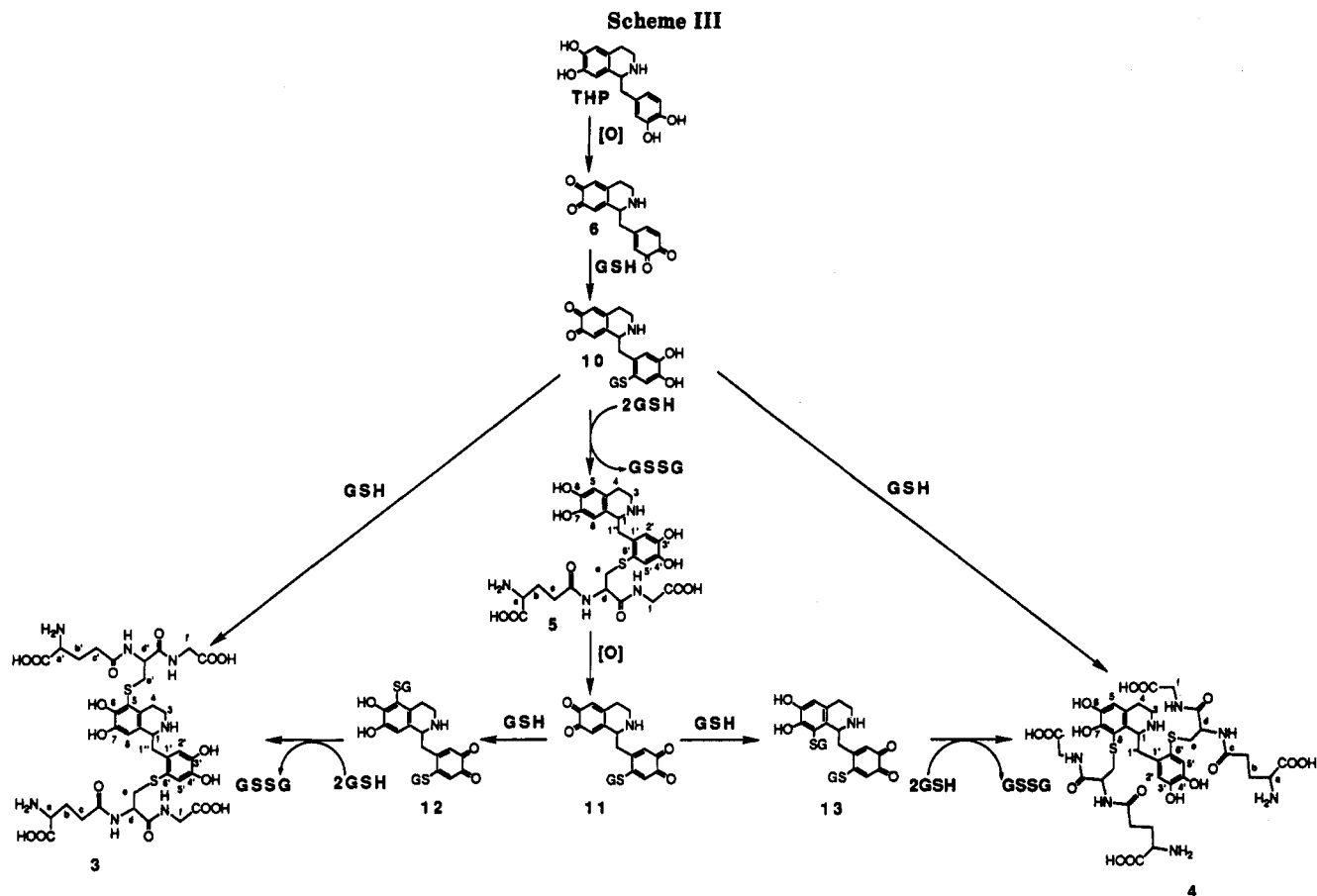
Previous investigators have established that THP has a very short half-life in the brain<sup>6</sup> and that it undergoes biotransformations both *in vitro* and *in vivo*.<sup>7</sup> It remains to be determined whether, in fact, THP can undergo oxidative transformations in the brain although the results reported here clearly indicate that the alkaloid is an easily oxidized compound and that a variety of oxidative enzyme systems catalyze this oxidation. Collins<sup>11</sup> has hypothesized

(21) Fa, Z.; Dryhurst, G. *Bioorg. Chem.*, in press.

(22) Nelson, J. M.; Dawson, C. R. *Advances in Enzymology*; Nord, F. F., Werkman, C. H., Eds.; Interscience Publishers: New York, 1964, Vol. 4, pp 99–151.

(23) Frieden, E.; Hsieh, H. S. *Advances in Enzymology*; Nord, F. F., Meister, A., Eds.; John Wiley & Son Publishers: New York, 1976; Vol. 44, pp 187–235.

(24) Walsh, C. *Enzymatic Reaction Mechanisms*; W. H. Freeman: San Francisco, 1979; pp 464–500.



that TIQ alkaloids elevated in the brain, as a result of ethanol consumption, might undergo oxidative transformations leading to toxins responsible for nerve damage. In the event that intraneuronal oxidations of THP do account for at least part of its biodegradation it seems reasonable to expect that diquinone 6 would be the proximate oxidation product. This compound is very reactive at physiological pH and reacts avidly with nucleophiles such as GSH to form several isolated glutathionyl conjugates, i.e., 3–5. Formation of these conjugates provides strong evidence that, if formed intraneuronally, diquinone 6 could possess toxic properties as a consequence of its expected reaction with cellular proteins. Indeed, alkylation and cross-linking of cellular proteins by highly electrophilic oxidation products of drugs such as 5,6- and 5,7-dihydroxytryptamine and 6-hydroxydopamine are widely believed to be the mechanisms by which these neurotoxins express their neurodegenerative effects *in vivo*.<sup>25,26</sup> Furthermore, GSH is an antioxidant/reductant which occurs intraneuronally in quite high concentrations (0.9–3.4 mM).<sup>27,28</sup> Accordingly, intraneuronal oxidations of THP would be expected to yield glutathionyl conjugates such as 3–5. Such reactions would act to deplete the tripeptide. Furthermore, it is not inconceivable that 3–5 might themselves possess toxic properties in the central nervous system. It is hoped to be able to report at some future time on the biological activities of conjugates 3–5. It is also likely that conjugates 3–5 might serve as analytical markers for *in vivo* oxidations of THP. The ease of

electrochemical oxidation of 3–5 would permit their analytical detection by HPLC with electrochemical detection, currently the most sensitive and selective method for the analysis of brain tissue.

### Experimental Section

Tetrahydropapaveroline hydrobromide (THP·HBr), tyrosinase (mushroom, EC 1.14.18.1), peroxidase (type VI from horseradish, EC 1.11.1.7), and glutathione were obtained from Sigma (St. Louis, MO). THP·HBr was purified by preparative HPLC (see later discussion); all other chemicals were used without further purification. Phosphate buffers of known ionic strength ( $\mu$ ) were prepared according to Christian and Purdy.<sup>29</sup>

Voltammograms were recorded at a pyrolytic graphite electrode (PGE; Pfizer Minerals, Pigments and Metals Division, Easton, PA) having a surface area of approximately 12.5 mm<sup>2</sup>. Equipment employed for voltammetry and controlled potential electrolyses has been described elsewhere.<sup>30</sup> All potentials are referred to the saturated calomel reference electrode (SCE) at ambient temperature 22 ± 2 °C.

High-performance liquid chromatography (HPLC) employed the binary gradient system described previously.<sup>30</sup> Reversed-phase preparative (J. T. Baker, Phillipsburg, NJ; C<sub>18</sub>, 10  $\mu$ m, 250 × 21 mm) and semipreparative (Brownlee Laboratories, Santa Clara, CA; RP-18, 5  $\mu$ m, 250 × 7 mm) columns were employed along with appropriate guard columns. Four mobile-phase solvents were used. Solvent A consisted of 3 mL of concentrated formic acid (HCOOH) and 3997 mL of deionized water. Solvent B was 6 mL of HCOOH, 1200 mL of HPLC-grade methanol (MeOH), 800 mL of HPLC-grade acetonitrile (MeCN), and 1994 mL of water. Solvent C was 4 mL of HCOOH and 3996 mL of water. Solvent D was 8 mL of HCOOH, 800 mL MeCN and 3192 mL of water. HPLC method I employed the preparative column with the following binary

(25) Singh, S.; Dryhurst, G. *J. Med. Chem.* 1990, 33, 3035–3044.

(26) Klemm, H. P.; Baumgarten, H. G.; Schlossberger, H. G. *J. Neurochem.* 1980, 35, 1400–1408.

(27) Mesina, J. E.; Page, R. H.; Hetzel, F. W.; Chopp, M. *Brain Res.* 1989, 478, 181–183.

(28) Slivka, A.; Mytilinou, C.; Cohen, G. *Brain Res.* 1987, 409, 275–284.

(29) Christian, G. D.; Purdy, W. C. *J. Electroanal. Chem. Interfacial Electrochem.* 1962, 3, 363–367.

(30) Singh, S.; Dryhurst, G. *J. Org. Chem.* 1990, 55, 1484–1489.

gradient: 0–30 min, linear gradient from 100% solvent A to 100% solvent B; 30–45 min, 100% solvent B. The flow rate was constant at 6 mL min<sup>-1</sup>. For HPLC method II the semipreparative column was used with the following binary gradient: 0–15 min, linear gradient from 100% solvent C to 100% solvent D; 15–25 min, 100% solvent D; flow rate 3 mL min<sup>-1</sup>.

**Electrochemical Oxidation Procedure and Product Isolation.** For a typical controlled potential electrooxidation and product isolation, 30 mL of 0.64 mM THP in pH 3.0 phosphate buffer ( $\mu = 0.15$ ) was electrolyzed at several plates of pyrolytic graphite (total surface area: ca. 150 cm<sup>2</sup>) at +0.46 V for 20 min. The reaction solution was vigorously bubbled with N<sub>2</sub> and stirred with a Teflon-coated magnetic stirring bar. The initially colorless solution changed to pale pink during the electrolysis. The entire 30 mL of product solution was injected onto the preparative reversed-phase HPLC column and separated using HPLC method I. The component eluted under HPLC peak 2 (Figure 3A) was collected and freeze-dried.

**Tyrosinase-Mediated Oxidation of THP in the Presence of Glutathione.** For preparative purposes 15 mL of pH 7.0 phosphate buffer ( $\mu = 0.15$ ) containing THP·HBr (4.0 mg; 0.7 mM), glutathione (16 mg; 3.5 mM), and tyrosinase (0.11 mg; 377 units) was stirred at room temperature for 3 h in a vessel open to the atmosphere. The entire 15-mL product solution was injected onto the preparative reversed-phase HPLC column and separated using HPLC method I. The components eluted under HPLC peaks 3–5 (Figure 8) were collected separately and freeze-dried. Compound 3 was dissolved in the minimum volume of water and purified using HPLC method II. Compound 4 was dissolved in the minimum volume of water and purified using HPLC method I. Compound 5 was purified using first HPLC method I, and the eluent was freeze-dried. The solid material was then dissolved in water and further purified using HPLC method II. The resulting solution was again freeze-dried.

**5,6-Dihydrodibenz[*b,g*]indolizine-2,3,9,10-tetrol (2).** Compound 2 was obtained as a very pale red solid. As noted earlier, the red color of isolated samples of 2 derives from its facile secondary oxidation.<sup>19,20</sup> Prolonged storage of a solid, dry sample of 2 on a freeze-drying apparatus, for example, resulted in the development of an increasingly intense red color; ultimately, a black polymeric solid was formed which was insoluble in all common solvents. Accordingly, the spectroscopic results for 2 reported below were obtained immediately after a chromatographically purified solution of the compound was freeze-dried. Compound 2 was very insoluble in D<sub>2</sub>O but was quite soluble in pyridine-*d*<sub>6</sub>. However, in the latter solvent a solution of 2 clearly decomposed over the course of a few hours, and hence, it was not possible to acquire a meaningful <sup>13</sup>C NMR spectrum. At pH 3.1 (33% MeCN)  $\lambda_{\max}$ , nm (log  $\epsilon_{\max}$ ): 310 (sh, 3.56), 292 (3.58), 220 (4.06), 206 (4.16). FAB-MS (3-nitrobenzyl alcohol matrix) gave  $m/e = 284$  (MH<sup>+</sup>, 16), 283 (M<sup>+</sup>, 100). Exact mass measurements on M<sup>+</sup> gave  $m/e = 283.0849$  (C<sub>16</sub>H<sub>13</sub>NO<sub>4</sub>; calcd  $m/e = 283.0844$ ). <sup>1</sup>H NMR (pyridine-*d*<sub>6</sub>):  $\delta$  7.52 (s, 1 H, C(4)-H), 7.28 (s, 1 H, C(1)-H), 7.15 (s, 1 H, C(8)-H), 7.07 (s, 1 H, C(11)-H), 6.77 (s, 1 H, C(12)-H), 3.93 (t,  $J = 6.3$  Hz, 2 H, C(6)-H<sub>2</sub>), 2.84 (t,  $J = 6.3$  Hz, 2 H, C(5)-H<sub>2</sub>). In order to confirm the structure of 2 the tetraacetate derivative was prepared as follows. Compound 2 (ca. 0.3 mg) was dissolved in acetic anhydride (6 mL), and pyridine (ca. 200  $\mu$ L) was added. The solution was stored under nitrogen at room temperature for 60 min and was then freeze-dried. The resulting residue was washed several times with cold water, centrifuged, and then dried under vacuum to give a white solid. FAB-MS (3-nitrobenzyl alcohol matrix) gave  $m/e = 452$  (MH<sup>+</sup>, 100). <sup>1</sup>H NMR (CDCl<sub>3</sub>):  $\delta$  7.51 (s, 1 H, C(4)-H), 7.38 (s, 1 H, C(1)-H), 7.16 (s, 1 H, C(8)-H), 7.12 (s, 1 H, C(11)-H), 6.77 (s, 1 H, C(12)-H), 4.20 (t,  $J = 6.5$  Hz, 2 H, C(6)-H<sub>2</sub>), 3.16 (t,  $J = 6.5$  Hz, 2 H, C(5)-H<sub>2</sub>), 2.34 (s, 3 H), 2.33 (s, 3 H), 2.32 (s, 3 H), 2.31 (s, 3 H). These spectral data are in complete accord with those expected for the 2,3,9,10-tetraacetyl derivative of 2 and agree with those reported by Mak and Brossi.<sup>20</sup>

**1,2,3,4-Tetrahydro-1-[(6-*S*-glutathionyl-3,4-dihydroxyphenyl)methyl]-5-*S*-glutathionyl-6,7-isoquinolinediol (3).** Compound 3 was isolated as a white solid. In pH 7.0 phosphate buffer the UV spectrum of 3 was:  $\lambda_{\max}$ , nm (log  $\epsilon_{\max}$ ) 282 (3.92), 206 (4.73). FAB-MS (thioglycerol-glycerol-water matrix) gave a pseudomolecular ion (MH<sup>+</sup>) at  $m/e = 898.2677$  (C<sub>36</sub>H<sub>48</sub>N<sub>2</sub>O<sub>16</sub>S<sub>2</sub>;

calcd  $m/e = 898.2599$ ). <sup>13</sup>C NMR (D<sub>2</sub>O):  $\delta$  177.50, 177.42, 177.34, 177.28, 177.19, 176.55, 176.49, 174.65, 149.67, 146.99, 146.83, 145.22, 134.17, 128.88, 126.47, 125.21, 124.00, 122.60, 118.58, 117.14, 58.36, 56.65, 56.01, 55.93, 55.47, 45.05, 41.08, 40.46, 37.50, 37.28, 34.20, 34.08, 28.81, 28.66, 28.43, 26.55. Thus, the <sup>13</sup>C NMR spectrum shows 36 resonances consisting of eight carbonyl carbon resonances of the two glutathionyl residues ( $\delta$  174.65 to 177.50), 12 resonances between  $\delta$  117.14 and 146.67 corresponding to the aromatic carbons of the THP residue, and 16 resonances between  $\delta$  26.55 and 58.36 due to the four aliphatic carbons of the THP residue and 12 aliphatic carbons of the two glutathionyl residues. Thus, 3 consists of two glutathionyl residues and one THP residues. <sup>1</sup>H NMR (D<sub>2</sub>O):  $\delta$  6.91 (s, 1 H, C(5')-H), 6.73 (s, 1 H, C(2')-H), 6.18 (s, 1 H, C(8)-H), 4.37 (m, 1 H, C(1)-H), 4.29–4.26 (m, 2 H, C(a)-H) and C(a')-H), 3.74 (t,  $J = 6.9$  Hz, 1 H, C(d)-H), 3.70–3.57 (m, 5 H, C(f)-H<sub>2</sub>, C(f')-H<sub>2</sub>, C(d')-H), 3.45–3.09 (m, 6 H, C(3)-H<sub>2</sub>, C(4)-H<sub>2</sub>, C(1'')-H<sub>2</sub>), 3.02–2.96 (m, 4 H, C(e)-H<sub>2</sub>, C(e')-H<sub>2</sub>), 2.49 (t,  $J = 6.9$  Hz, 2 H, C(c)-H<sub>2</sub>), 2.40–2.37 (m, 2 H, C(c')-H<sub>2</sub>), 2.10 (td,  $J = 6.9$  Hz, 2 H, C(b)-H<sub>2</sub>), 2.03–1.96 (m, 2 H, C(b')-H<sub>2</sub>).

**1,2,3,4-Tetrahydro-1-[(6-*S*-glutathionyl-3,4-dihydroxyphenyl)methyl]-8-*S*-glutathionyl-6,7-isoquinolinediol (4).** Compound 4 was isolated as a white solid. In pH 7.0 phosphate buffer the UV spectrum of 4 was:  $\lambda_{\max}$ , nm (log  $\epsilon_{\max}$ ) 278 (4.0), 204 (4.66). FAB-MS (thioglycerol-glycerol-water matrix) gave a pseudomolecular ion (MH<sup>+</sup>) at  $m/e = 898.2659$  (10%; C<sub>36</sub>H<sub>48</sub>N<sub>2</sub>O<sub>16</sub>S<sub>2</sub>; calcd  $m/e = 898.2599$ ). <sup>13</sup>C NMR (D<sub>2</sub>O):  $\delta$  177.80, 177.67, 177.49, 177.28, 176.55, 176.50, 174.55, 174.41, 149.65, 146.88, 146.72, 145.40, 134.05, 128.39, 126.49, 125.33, 124.11, 122.43, 118.61, 116.83, 58.48, 56.67, 56.47, 55.45, 45.35, 45.25, 41.55, 41.32, 40.33, 37.65, 37.43, 34.02, 33.96, 28.77, 28.58, 26.62. The <sup>13</sup>C NMR spectrum thus exhibits 36 resonances consisting of eight carbonyl carbon resonances ( $\delta$  177.80 to 174.41) corresponding to two glutathionyl residues, 12 resonances between  $\delta$  149.65 and 116.83 corresponding to the aromatic carbons of one THP residue, and 16 resonances between  $\delta$  58.48 and 26.62 due to four aliphatic carbons of one THP residue and 12 aliphatic carbons of two glutathionyl residues. Thus, 4 consists of two glutathionyl residues and one THP residue. <sup>1</sup>H NMR (D<sub>2</sub>O):  $\delta$  6.98 (s, 1 H, C(5')-H), 6.74 (s, 1 H, C(2')-H), 6.34 (s, 1 H, C(5)-H), 4.55 (t,  $J = 7.2$  Hz, 1 H, C(1)-H), 4.40–4.32 (m, 2 H, C(a)-H, and C(a')-H), 3.72 (t,  $J = 6.5$  Hz, 1 H, C(d)-H), 3.67–3.57 (m, 5 H, C(f)-H<sub>2</sub>, C(f')-H<sub>2</sub>, C(d')-H), 3.45–3.34 (m, 2 H, C(3)-H<sub>2</sub>), 3.22–2.95 (m, 8 H, C(e)-H<sub>2</sub>, C(e')-H<sub>2</sub>, C(1'')-H<sub>2</sub>, C(4)-H<sub>2</sub>), 2.48 (t,  $J = 7.5$  Hz, 2 H, C(c)-H<sub>2</sub>), 2.39–2.20 (m, 2 H, C(c')-H<sub>2</sub>), 2.0–9 (td,  $J = 7.2$  Hz, 2 H, C(b)-H<sub>2</sub>), 2.01–1.90 (m, 2 H, C(b')-H<sub>2</sub>).

**1,2,3,4-Tetrahydro-1-[(6-*S*-glutathionyl-3,4-dihydroxyphenyl)methyl]-6,7-isoquinolinediol (5).** Compound 5 was isolated as a white solid. In pH 7.0 phosphate buffer the UV spectrum of 5 was:  $\lambda_{\max}$ , nm (log  $\epsilon_{\max}$ ) 288 (3.72), 204 (4.66). FAB-MS (3-nitrobenzyl alcohol matrix) gave  $m/e = 593.1947$  (MH<sup>+</sup>, 5%; C<sub>26</sub>H<sub>33</sub>N<sub>4</sub>O<sub>4</sub>S, calcd  $m/e = 593.1917$ ). <sup>13</sup>C NMR (D<sub>2</sub>O)  $\delta$  178.52, 177.43, 176.60, 174.22, 147.35, 147.01, 146.79, 145.52, 130.31, 128.96, 126.54, 125.70, 122.29, 120.01, 118.51, 116.67, 58.58, 56.78, 55.78, 45.86, 41.88, 41.10, 37.58, 34.11, 28.82, 26.72. The resonances between  $\delta$  178.52 and 174.22 correspond to four carbonyl carbons of one glutathionyl residue. The resonances between  $\delta$  147.35 and 116.67 correspond to the 12 aromatic carbons of one THP residue. The resonances between  $\delta$  58.58 and 26.72 correspond to the four aliphatic carbons of the THP residue and six aliphatic carbons of the glutathionyl residue. Thus, 5 consists of one residue each of THP and glutathione. <sup>1</sup>H NMR (D<sub>2</sub>O):  $\delta$  6.83 (s, 1 H, C(5')-H), 6.77 (s, 1 H, C(2')-H), 6.74 (s, 1 H, C(5)-H), 6.61 (s, 1 H, C(8)-H), 4.64–4.60 (m, 1 H, C(1)-H), 4.38 (m, 1 H, C(a)-H), 3.74–3.64 (m, 3 H, C(f)-H<sub>2</sub>, C(d)-H), 3.50–3.40 (m, 1 H, C(3)-H), 3.35–3.25 (m, 3 H, C(3)-H and C(1'')-H<sub>2</sub>), 3.19–3.11 (m, 1 H, C(4)-H), 3.04–2.91 (m, 3 H, C(4)-H, C(e)-H<sub>2</sub>), 2.45 (t,  $J = 7.5$  Hz, 2 H, C(c)-H<sub>2</sub>), 2.07 (td,  $J = 7.5$  Hz,  $J = 7.5$  Hz, 2 H, C(b)-H<sub>2</sub>). The absence of either short-range coupling between the C(5') and C(6') protons or long-range coupling between the C(6') and C(2') protons in 5 and the fact that the C(5')-H and C(2')-H resonances are singlets clearly indicates that the glutathionyl residue is linked at the C(6') position.

**Acknowledgment.** This work was supported by National Institutes of Health Biomedical Research Support Grant No. SO7 RR070078. Additional support was pro-



vided by the Research Council and Vice Provost for Research Administration at the University of Oklahoma.

Registry No. 2, 73053-76-6; 3, 137007-57-9; 4, 137007-58-0; 5, 137007-59-1; THP-HBr, 16659-88-4; GSH, 70-18-8; tyrosinase,

9002-10-2; ceruloplasmin, 9031-37-2; peroxidase, 9003-99-0.

Supplementary Material Available:  $^{13}\text{C}$  NMR spectra and high-resolution FAB-MS data for 3-5 (3 pages). Ordering information is given on any current masthead page.

## Evidence for an Intramolecular, Stepwise Reaction Pathway for PEP Phosphomutase Catalyzed P-C Bond Formation

Michael S. McQueney, Sheng-lian Lee, William H. Swartz, Herman L. Ammon, Patrick S. Mariano,\* and Debra Dunaway-Mariano\*

Department of Chemistry and Biochemistry, University of Maryland, College Park, Maryland 20742

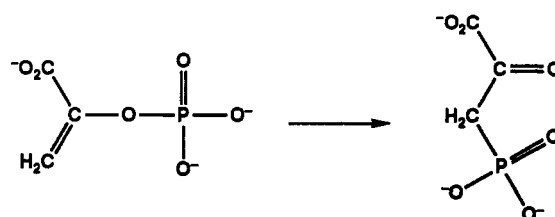
Received June 12, 1991

The *Tetrahymena pyriformis* enzyme, phosphoenolpyruvate phosphomutase, catalyzes the rearrangement of phosphoenolpyruvate to the P-C bond containing metabolite, phosphonopyruvate. To distinguish between an intra- and intermolecular reaction pathway for this process an equimolar mixture of  $[\text{P-}^{18}\text{O}, \text{C}(2)\text{-}^{18}\text{O}]$  thiophosphonopyruvate and (all  $^{16}\text{O}$ ) thiophosphonopyruvate was reacted with the phosphomutase, and the resulting products were analyzed by  $^{31}\text{P}$  NMR. The absence of the cross-over product  $[\text{C}(2)\text{-}^{18}\text{O}]$  thiophosphoenolpyruvate in the product mixture was interpreted as evidence for an intramolecular reaction pathway. To distinguish between a concerted and stepwise intramolecular reaction pathway the pure enantiomers of the chiral substrate  $^{18}\text{O}$ -thiophosphonopyruvate were prepared and the stereochemical course of their conversion to chiral  $^{18}\text{O}$ -thiophosphoenolpyruvate was determined. The assignments of the phosphorus configurations in the  $^{18}\text{O}$ -thiophosphonopyruvate enantiomers reported earlier (McQueney, M. S.; Lee, S.-l.; Bowman, E.; Mariano, P. S.; Dunaway-Mariano, D. *J. Am. Chem. Soc.* 1989, 111, 6885-6887) were revised according to the finding that introduction of the  $^{18}\text{O}$  label into the thiophosphonopyruvate precursor occurs with retention rather than with (the previously assumed) inversion of configuration. On the basis of the observed conversion of  $(S_p)$ - $^{18}\text{O}$ -thiophosphonopyruvate to  $(S_p)$ - $^{18}\text{O}$ -thiophosphoenolpyruvate and  $(R_p)$ - $^{18}\text{O}$ -thiophosphonopyruvate to  $(R_p)$ - $^{18}\text{O}$ -thiophosphoenolpyruvate, it was concluded that the PEP phosphomutase reaction proceeds with retention of the phosphorus configuration and therefore by a stepwise mechanism. Lastly, the similar reactivity of the oxo- and thio-substituted phosphonopyruvate substrates (i.e., nearly equal  $V_{\text{max}}$ ) was interpreted to suggest that nucleophilic addition to the phosphorus atom is not rate limiting among the reaction steps.

### Introduction

The chemistry of P-C bond formation in biological systems has eluded researchers since the discovery of the first phosphonate natural product over 30 years ago.<sup>1</sup> Laboratory chemical synthesis of P-C linkages typically involve the addition of a nucleophilic phosphorus reactant to a carbon electrophile. If such a strategy were to be used in a biological system, precursors containing phosphorus in the +3 oxidation state would be required. An alternate mode of P-C bond formation might rely on the activation of a carbon acid for nucleophilic addition to the phosphorus atom of a phosphate ester or anhydride. While this latter approach is analogous to the phosphoryl transfer strategy employed in the biosynthesis of organophosphates,<sup>2</sup> the low acidity of carbon acids (as opposed to oxy acids) and the comparatively high energy of the P-C vs P-O bond<sup>3</sup> would pose a particular challenge to the protein catalyst.

Recently, the P-C bond forming enzyme phosphoenolpyruvate (PEP)<sup>4</sup> phosphomutase was isolated in our laboratory from the protozoan, *Tetrahymena pyriformis*.<sup>5</sup> This enzyme catalyzes the rearrangement of PEP to phosphonopyruvate, a reaction which serves as a major entry step into the phosphonate class of natural products.<sup>6,7</sup>



The present study examines the chemical mechanism of this enzymic reaction in the thermodynamically favored,

(1) For reviews, see: Hilderbrand, R. L., Ed. *The Role of Phosphonates in Living Systems*; CRC Press: Boca Raton, 1983. Hori, T.; Horiguchi, M.; Hayschi, A. in *Biochemistry of Natural C-P Compounds*; Maruzen: Tokyo, 1984. Mastalerz, P. *Natural Products Chemistry*; Zaleski, R. I., Skolik, J. J., Eds.; Elsevier: Amsterdam, 1984.

(2) For a review, see: Knowles, J. R. *Annu. Rev. Biochem.* 1980, 49, 877.

(3) Hartley, S. B.; Holmes, W. S.; Jacques, J. K.; Mole, M. F.; McCoubrey, J. C. *Quart. Rev.* 1963, 17. Van Wazer, J. R. *Phosphorus and Its Compounds*; Interscience Publishers, Inc.: New York, 1951; p 887.

(4) Abbreviations: NAD<sup>+</sup>, nicotinamide adenine dinucleotide; NADH, dihydronicotinamide adenine dinucleotide; Hepes, N-(2-hydroxyethyl)piperazine-N'-2-ethanesulfonic acid; PEP, phosphoenolpyruvate; AMP, adenosine 5'-monophosphate; ADP, adenosine 5'-diphosphate; ATP, adenosine 5'-triphosphate; ATP $\beta$ S, adenosine 5'-(1-thiotriphosphate); ATP $\gamma$ S, adenosine 5'-(2-thiotriphosphate); ADP $\beta$ S, adenosine 5'-(2-thiodiphosphate); EDTA (ethylenedinitrilo)tetraacetic acid; p-TsOH, p-toluenesulfonic acid; TEAB, triethylamine bicarbonate; Tris, tris(hydroxymethyl)aminomethane; THF, tetrahydrofuran; HPLC, high-pressure liquid chromatography; NMR, nuclear magnetic resonance.

\* To whom correspondence should be addressed.